



ELSEVIER

Journal of Crystal Growth 156 (1995) 163–168

JOURNAL OF **CRYSTAL
GROWTH**

Heterogeneous nucleation of planar defects in Mn-doped ZnSe/GaAs

S.I. Molina ^{*,1}, P.D. Brown, C.J. Humphrey

Department of Materials Science and Metallurgy, University of Cambridge, Pembroke Street, Cambridge CB2 3QZ, UK

Received 27 January 1995; manuscript received in final form 30 May 1995

Abstract

A heterogeneous source for the nucleation of inclined planar defects within a Mn-doped ZnSe/GaAs epitaxial layer grown by metalorganic vapour phase epitaxy is identified as MnSe particles at the ZnSe/GaAs interface (it is possible that the particles contain up to 6% Zn). The MnSe particles have the rock-salt crystal structure and are randomly distributed along the interface. The planar defects emanate from the rough interface between ZnSe and the particles and nucleation is probably mediated by the 3.8% lattice misfit between ZnSe and MnSe.

1. Introduction

One of the most promising heterostructures for optoelectronic applications in the blue region of the spectrum is ZnSe/GaAs [1] as the ZnSe semiconductor possesses a room-temperature direct band-gap of 2.7 eV. The incorporation of paramagnetic Mn^{2+} ions to form (Zn,Mn)Se is particularly interesting in view of the possibility of forming magnetically tuneable quantum well structures [2,3]. Zincblende ZnSe and $Zn_xMn_{1-x}Se$ exhibit many interesting physical properties which are being increasingly studied [4,5].

Despite the low lattice misfit between ZnSe and GaAs (0.25% at room temperature), inclined

planar defects are commonly observed to thread the ZnSe epilayer [6–9] and these defects can degrade the optoelectronic properties of devices [10]. Sources for the nucleation of dislocations have been described in ZnSe/GaAs [11] but no clear evidence has been presented to explain the nucleation of microtwins in these heterostructures.

In this study the interfacial defect microstructure of Mn-doped ZnSe/(001)GaAs is examined in detail and interfacial particulates responsible for the introduction of microtwins are identified as $Zn_xMn_{1-x}Se$ ($x \leq 0.06$) with the rock-salt crystal structure.

2. Experimental procedure

A 1.6 μm ZnSe epitaxial layer doped nominally with 1% Mn was grown on a GaAs(001) substrate at 275°C by metalorganic vapour phase

* Corresponding author.

¹ Permanent address: Departamento de Ciencia de los Materiales e IM y QI, Universidad de Cádiz, Apdo. 40 11510 Puerto Real (Cádiz), Spain.

epitaxy (MOVPE) in a manner similar to that previously described [12,13]. The substrate was annealed at 600°C prior to growth. TEM foils were prepared by sequential mechanical polishing and Ar⁺ ion milling. The defect microstructure was examined by conventional transmission electron microscopy (TEM) and high resolution electron microscopy (HREM) using Philips CM30 and Jeol 4000EX Mark II transmission electron microscopes, respectively. The HREM images were compared with simulations obtained using the EMS software [14] running on a Silicon Graphics Workstation. Compositional variations were characterised by energy dispersive X-ray (EDX) spectroscopy using a VG HB501 scanning transmission electron microscope with a probe size of 1 nm. Spectra were acquired and analyzed using the LINK Analytical AN10000 system. Selected area electron diffraction (SAED) was used to detect possible structural changes in the epilayer, while absolute crystal polarity and misorientation between epilayer and substrate were ascertained using convergent beam electron diffraction (CBED) [15,16].

3. Results and discussion

The distribution of planar defects in the epilayer is shown in the cross-sectional TEM image of Fig. 1. A large number of microtwins ($\sim 30 \mu\text{m}^{-1}$ at 100 nm from the interface) propagate through the epilayer, although no threading dislocations were observed (which is consistent with a density of $\leq 10^6 \text{ cm}^{-2}$). The density of planar defects decreases with distance away from the interface following interactions between defects propagating along different $\langle 112 \rangle$ directions.

3.1. The nature of the interfacial phase

Planar defects are seen to emanate from several distinctive features decorating the interface and are not uniformly generated along its length, as illustrated by the 002-bright- and dark-field images shown in Figs. 2a and 2b, respectively. These interfacial inclusions appear bright with respect to ZnSe and GaAs in the dark-field im-



Fig. 1. Bright-field cross-sectional TEM image showing the distribution of inclined planar defects within the ZnSe:Mn epilayer.

age. The $\langle 110 \rangle$ SAED patterns recorded from the GaAs substrate, the interfacial phase and the ZnSe epilayer are similar, but demonstrate that the interfacial phase has a slightly smaller lattice parameter than GaAs. Extra spots in the ZnSe pattern were also present due to the twins in the epilayer.

EDX spectra acquired using a 1 nm electron probe from different regions and thicknesses of the sample are shown in Fig. 3. Spectra obtained from GaAs and ZnSe:Mn regions close to the interfacial inclusions were used as a reference for the compositional calculations, while spectra acquired from regions distributed throughout the specimen were used to elucidate the effect of sample thickness on the spectra and to eliminate possible artefacts from the ion milling preparation procedure. Spectra 1 to 3 were recorded

across an interfacial particle as indicated in the schematic diagram and correspond to a relatively thick region of the specimen. Conversely, spectrum 5 was acquired from an interfacial particle situated in a thin region of the specimen. Spectrum 4 is recorded from a region close to the ZnSe:Mn/GaAs interface which does not exhibit any discernible contrast due to interfacial phase formation. Consideration of the spectra highlights two important results. Firstly, no Mn is detected in the epilayer away from the interfacial particulates (to the limit of the EDX technique), and

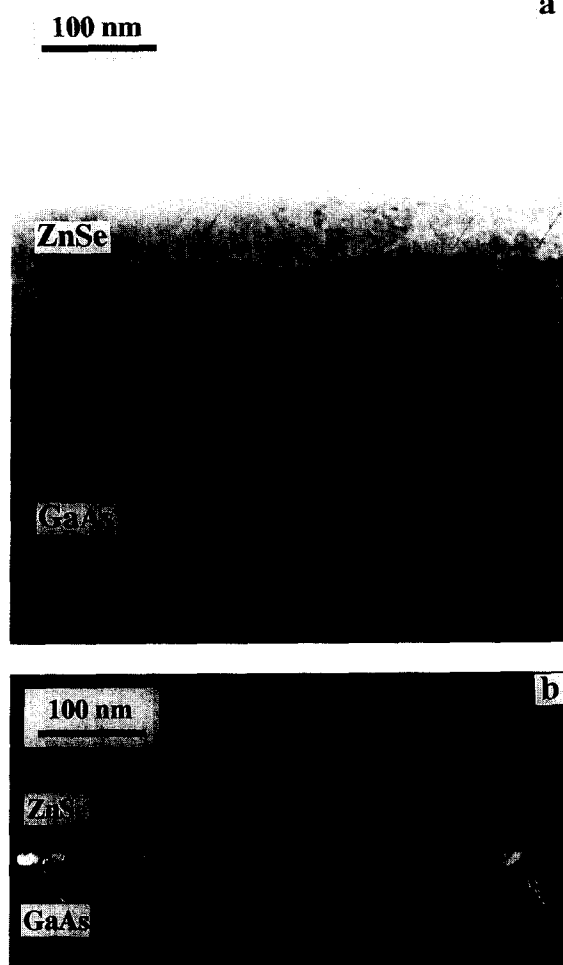


Fig. 2. (a) 002-bright-field and (b) 002-dark-field TEM images illustrating the strong contrast associated with the interfacial particles from which the planar defects emanate (arrowed).

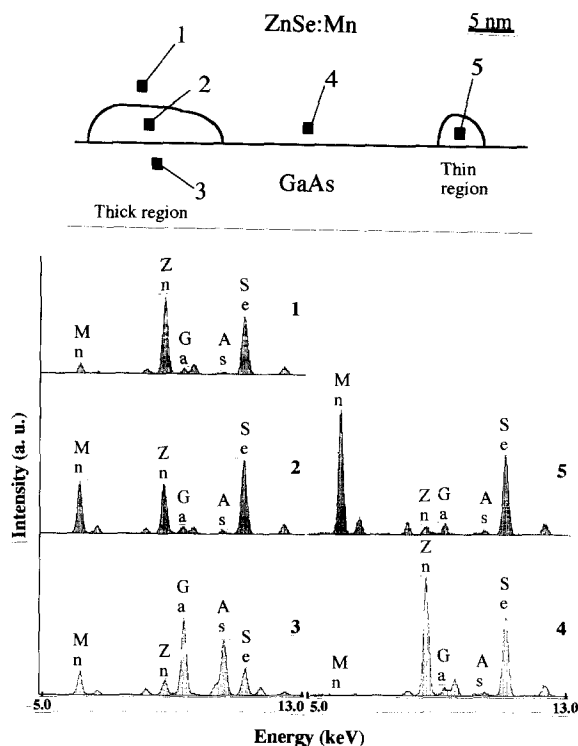


Fig. 3. A series of EDX spectra acquired (1–3) from a thick region of the sample across an interfacial particle; (4) from a region near the ZnSe:Mn/GaAs interface which exhibited no interfacial phase contrast; and (5) from a thin region of the specimen containing an interfacial particle. The labelled peaks correspond to $K\alpha$ radiation with each element indicated.

along the length of the generated planar defects in particular; and secondly the Zn content in the interfacial phase in the very thin region of the TEM foil is negligible, demonstrating that Mn is highly concentrated within this interfacial compound. The simplest known stoichiometries for a compound containing Mn and Se are $MnSe$ and $MnSe_2$ [17]. The quantity of detected Se in the unknown phase suggests that it is probably $MnSe$. The detection of a small amount of Zn in the particulates is probably due to beam broadening, scattering effects or background scintillation, for example, although the possibility of low Zn content $Zn_xMn_{1-x}Se$ formation cannot be disregarded. Similarly, the very small quantities of Ga and As detected in the interfacial phase are probably due to artefacts of the EDX procedure.

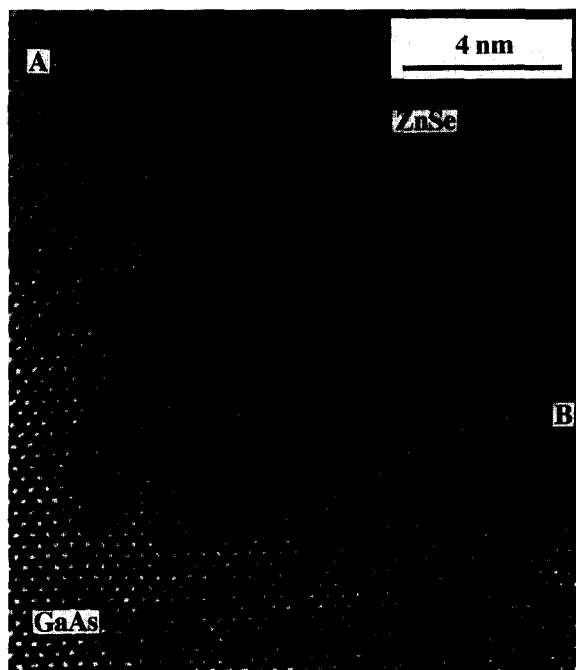


Fig. 4. HREM image recorded along $[110]$ showing an interfacial particle. Stacking fault A emanates from the ZnSe/particle boundary. Stacking fault B is contained within the interfacial particle.

Fig. 4 shows a $\langle 110 \rangle$ HREM image of an interfacial particle and these ranged in size between 4 and 16 nm along the $\langle 001 \rangle$ growth direction. Measurement of image spacings suggested a lattice parameter for the unknown compound of 0.548 ± 0.004 nm, assuming a cubic structure, as compared with 0.56532 and 0.56676 nm for GaAs and ZnSe, respectively, and a smaller value is consistent with the earlier indications of SAED. Some dislocations were present at the interface between the interfacial compound and the GaAs.

Absolute sample polarity was determined in situ using CBED and confirmed no polarity change across the epilayer/substrate interface as expected. However, these measurements also in-

dicated a small misorientation between the epilayer and substrate around the $[001]$ and $[1\bar{1}0]$ directions of magnitude ≤ 1 mrad in both cases. This misorientation is attributed to the non-uniform distribution of interfacial particles and the associated planar defects threading the epilayer.

The combined SAED, HREM and EDX data demonstrate that the interfacial phase is MnSe (or low Zn content $\text{Zn}_x\text{Mn}_{1-x}\text{Se}$) and is cubic in structure. There are two known cubic phases of MnSe [17,18], i.e. α -MnSe and β -MnSe, and the relevant crystal structure data [17–20] is summarised in Table 1. X-ray [21] and electron [22] diffraction studies indicate that α -MnSe films have the rock-salt crystal structure, and epitaxial MnSe grown by pulsed-laser deposition is known to adopt this structure [5]. Conversely, the epitaxial growth of sphalerite MnSe has been demonstrated by molecular beam epitaxy [23]. The MnSe phase identified in this MOVPE grown sample is not of the sphalerite structure for three reasons. Firstly, sphalerite β -MnSe has a larger lattice parameter than ZnSe or GaAs, while the measured value for the interfacial particle is smaller; secondly, the calculated intensity of the 002 reflection from β -MnSe using dynamical diffraction theory is similar or only slightly larger than that of ZnSe or GaAs, while experimentally it is clearly larger since the particles appear bright in the 002 dark-field image; and thirdly, simulations based on the sphalerite structure do not compare with the HREM images of the interfacial phase. On the other hand, the formation of rock-salt α -MnSe is consistent with all these observations. Its lattice parameter (0.54626 nm) agrees favourably with that measured by HREM (0.548 ± 0.004 nm). The calculated intensity of the 002 reflection is much larger for this structure than that for ZnSe or GaAs, and Bloch wave calculations to emphasise this are shown in Fig. 5, and this explains why the particulates appear bright in the 002 dark-field

Table 1
Crystal structure data for cubic MnSe

Phase	Space group	Structure prototype	a (nm)
α -MnSe	$\text{Fm}\bar{3}\text{m}$	NaCl (rock salt)	0.54626 ± 0.00005 [19]
β -MnSe	$\text{F}\bar{4}3\text{m}$	ZnS (sphalerite)	0.58935 ± 0.00075 [20]

images. Also, the HREM images recorded from the interfacial phase are consistent with rock-salt α -MnSe. Fig. 6 compares two images recorded at different defocii with simulations obtained using the multislice algorithm. Simulations for rock-salt $\text{Zn}_x\text{Mn}_{1-x}\text{Se}$ ($x = 0$ to 1) demonstrated it is not possible to distinguish between $\text{Zn}_x\text{Mn}_{1-x}\text{Se}$ or α -MnSe as the interfacial phase. Taking the lattice parameter of rock-salt ZnSe as 0.508 nm [24] and assuming Vegard's law, then the measured HREM lattice parameter could possibly indicate a Zn content of $\leq 6\%$. However, since the particles are strained, and there are thin foil surface relaxation effects, it is suggested that the probable composition of the particles is MnSe. It is noted that a transition from sphalerite ZnSe to rock-salt ZnSe at room temperature would require high pressure (≥ 100 kbar) [24–26]. To summarise, the interfacial compound is determined to be $\text{Zn}_x\text{Mn}_{1-x}\text{Se}$ ($x \leq 0.06$) with the rock-salt crystal structure, and probably MnSe.

3.2. Heterogeneous nucleation of planar defects

HREM images recorded for [110] demonstrate that stacking disorders contained within the inter-

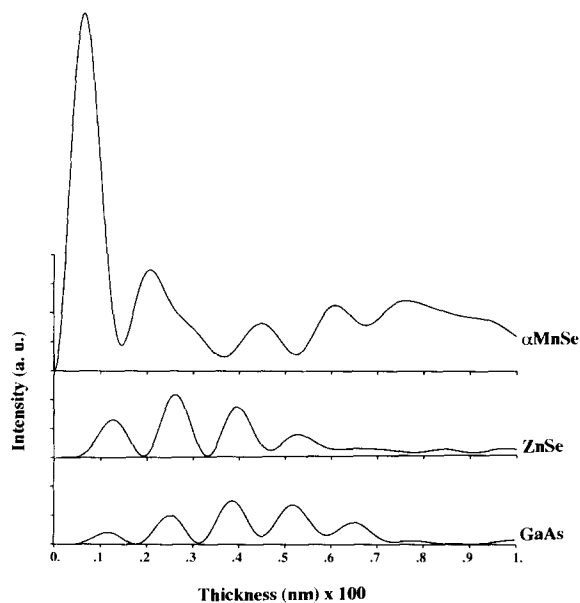


Fig. 5. Calculated intensities of the 002 reflection against specimen thickness using the Bloch wave formalism for α -MnSe, GaAs and ZnSe.

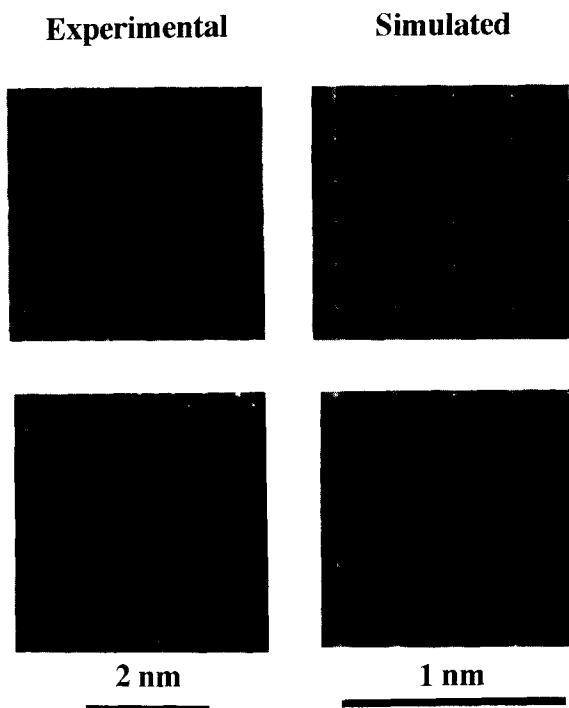


Fig. 6. Experimental and simulated HREM images of the contrast exhibited by the interfacial particles. The simulated image is of rock-salt α -MnSe. Defocus (underfocus) of the upper part is 30 ± 2 nm, and of the lower part is 62 ± 2 nm. Specimen thickness is 7 ± 1 nm.

facial phase have partial dislocations located at the α -MnSe/GaAs and ZnSe/ α -MnSe interfaces. However, planar defects nucleated at the ZnSe/ α -MnSe boundary are seen to propagate through the ZnSe epilayer (as illustrated by Fig. 4). The rough nature of the ZnSe/ α -MnSe boundary suggests that planar defects are nucleated at boundary steps and mediated by the strain arising from the 3.8% lattice misfit between ZnSe and α -MnSe. Hence, this interface is identified as the nucleation site for the inclined planar defects threading the ZnSe epilayer.

4. Conclusion

An epitaxial layer of ZnSe doped with 1% Mn grown by MOVPE on GaAs(001) has been studied. The Mn was found to segregate to the

ZnSe/GaAs interface and form particles identified as MnSe having the rock-salt crystal structure. These particles may contain up to 6% Zn, i.e. be $Zn_xMn_{1-x}Se$, with $x \leq 0.06$, and are randomly distributed along the interface. The boundary between ZnSe and the particles is shown to be the source of inclined planar defects threading through the ZnSe epilayer.

Acknowledgements

S.I.M. would like to acknowledge NATO for funding this work through a postdoctoral scholarship. P.D.B. wishes to acknowledge SERC for funding under grant GR/J37966. The authors would like to thank Dr. A.P.C. Jones for providing the sample used in this study, Dr. G.S. Chen for assistance during the acquisition of EDX/STEM data and Dr. C.J.D. Hetherington for Jeol 4000 EX HREM instruction.

References

- [1] R.M. Park, M.B. Troffer, C.M. Rouleau, J.M. DePuydt and M.A. Haase, *Appl. Phys. Lett.* 57 (1990) 2127.
- [2] J.K. Furdyna, *J. Appl. Phys.* 64 (1988) R29.
- [3] O. Goede and W. Heimbrod, *Phys. Status Solidi (b)* 146 (1988) 11.
- [4] P.M. Lee, A. Kisiel, E. Burattini and M. Demianiuk, *J. Phys. Condens. Matter.* 6 (1994) 5771.
- [5] J. Misiewicz, C. Huber, D. Heiman and T.Q. Wu, *Appl. Surf. Sci.* 69 (1993) 156.
- [6] F.A. Ponce, W. Stutius and J.W. Werthen, *Thin Solid Films* 104 (1983) 133.
- [7] W. Stutius and F.A. Ponce, *J. Appl. Phys.* 58 (1985) 1548.
- [8] J. Petruzzello, J. Gaines, P. van der Sluis, D. Olego and C. Ponzoni, *Appl. Phys. Lett.* 62 (1993) 1496.
- [9] L.H. Kuo, L. Salamanca-Riba, J.M. DePuydt, H. Cheng and J. Qiu, *Appl. Phys. Lett.* 63 (1993) 3197.
- [10] Y. Chen, X. Liu, E. Weber, E.D. Bourret, Z. Liliental-Weber, E.E. Haller, J. Washburn, D.J. Olego, D.R. Dorman, J.M. Gaines and N.R. Tasker, *Appl. Phys. Lett.* 65 (1994) 549.
- [11] L.K. Kuo, L. Salamanca-Riba, J.M. DePuydt, H. Cheng and J. Qiu, *Philos. Mag. A* 69 (1994) 301.
- [12] A.C. Wright and B. Cockayne, *J. Crystal Growth* 68 (1984) 233.
- [13] A.P.C. Jones, A.W. Brinkman, G.J. Russell, J. Woods, P.J. Wright and B. Cockayne, *J. Crystal Growth* 79 (1986) 729.
- [14] P.A. Stadelmann, *Ultramicroscopy* 21 (1987) 131.
- [15] J. Taftø and C.J.H. Spence, *J. Appl. Cryst.* 15 (1982) 60.
- [16] K. Ishizuka and J. Taftø, *Acta Cryst. B* 40 (1984) 332.
- [17] T.B. Massalski, Ed., *Binary Alloy Phase Diagrams*, Vol. 3 (ASM Int., 1990).
- [18] P. Villars and L.D. Calvert, Eds., *Pearson's Handbook of Crystallographic Data for Intermetallic Phases*, Vols. 1–3 (Am. Soc. Metals, Metals Park, OH, 1985).
- [19] W.R. Cook, Jr., *J. Am. Ceram. Soc.* 51 (1968) 518.
- [20] P.R. Bressler, Th. Klöpper and H.-E. Gumlich, *J. Vac. Sci. Technol. B* 11 (1993) 1621.
- [21] V. Thanigaimani, PhD Thesis, Univ. of West Indies, St. Augustine, 1993.
- [22] P. Singh, *Indian J. Pure Appl. Phys.* 18 (1980) 950.
- [23] R.L. Gunshor, A.V. Nurmikko, L.A. Kolodziejski, M. Kobayashi and N. Otsuka, *J. Crystal Growth* 101 (1990) 14.
- [24] P.L. Smith and J.E. Martin, *Phys. Lett.* 19 (1965) 541.
- [25] G.A. Samara and H.G. Drickamer, *J. Phys. Chem. Solids* 23 (1962) 457.
- [26] G.J. Piermarini and S. Block, *Rev. Sci. Instrum.* 46 (1975) 973.